Наносистеми, наноматеріали, нанотехнології
Nanosistemi, Nanomateriali, Nanotehnologii
2026, т. 24, № 1, сс. 115–122
https://doi.org/10.15407/nnn.24.01.0115

PACS numbers: 61.05.cp, 78.30.Hv, 78.55.Hx, 78.67.Bf, 81.07.Bc, 81.70.Pg

Preparing of Sb:SrF_2 Nanoparticles and Studying Their Structural and Luminescence Properties

Ahmad Khoudro[1], Mufid Diab[2], and Omar Al-Aboush[1]

[1]*Department of Physics,*
Faculty of Science,
Tishreen University,
Latakia, Syria
[2]*Department of Physics,*
Faculty of Science,
AL-Baath University,
Homs, Syria

In this research, strontium fluoride doped with antimony in different proportions is prepared using solid-state method. The prepared compounds are characterized using XRD, FT-IR and photoluminescence techniques. As found, the prepared compounds crystallize according to the cubic pattern with nanosize grains and have a clear fluorescence property.

У цьому дослідженні фторид Стронцію, леґований Стибієм у різних пропорціях, був одержаний твердофазним методом. Одержані сполуки було охарактеризовано за допомогою методів рентґенівської дифракції (XRD), інфрачервоної спектроскопії на основі Фур'є-перетвору (FT-IR) та фотолюмінесценції. Було виявлено, що одержані сполуки кристалізуються у кубічну структуру із нанорозмірними зернами, а також мають чітку флюоресцентну властивість.

Key words: strontium fluoride, doping, SrF_2:Sb, photoluminescence.

Ключові слова: фторид Стронцію, леґування, SrF_2:Sb, фотолюмінесценція.

(Received 14 November, 2024; in revised form, 22 November, 2024)

1. INTRODUCTION

Since the first Nd:YAG laser ceramic was reported by Ikesue *et al.* in 1995 [1], transparent polycrystalline ceramics have found increased interest over the last few years. The majority of transpar-

ent ceramics researches focus on oxide materials like $Nd_{3x}Y_{3-3x}Al_5O_{12}$ (Nd:YAG), however, fluoride materials are very attractive and promising materials for laser applications [2–5]. Among the fluoride compounds, strontium fluoride (SrF_2) is an attractive material. Because of its excellent optical properties, *e.g.*, the high transmission in the infrared and ultraviolet spectral range 0.13–11 μm, the low refractive index nDj1.439 and 589 nm, and the extremely low solubility in water 120 mg L1, SrF_2 is an ideal material for optical applications and is often used as a coating material for high-quality optical windows, prisms and lenses to reduce reflection and to increase transmission. Furthermore, as the isotype of CaF_2, SrF_2 has gained great interest as a laser material when doped with rare-earth ions [6–8].

For example, thanks to its broad emission bands, Yb:SrF_2 single crystal is a promising gain medium in tuneable laser and ultra-short pulse laser generator [9, 10]. With their superior optical and chemical properties, SrF_2 ceramics are highly suitable for a wide range of industrial and scientific applications such as laser technology, scintillators, photolithographic processing and specialized window production. However, few works have been done on the preparation of SrF_2 transparent ceramics. Basiev *et al.* reported laser operation of rare-earth doped ceramics of Nd:SrF_2 and its solid solutions fabricated by a hot-forming method [11]. However, it is deformation of single crystals and lacks for advantages of ceramics such as much superior mechanical property, lower temperatures than single crystal growth process.

In this study, we have focused on preparation of SrF_2 nanopowders doped with Sb.

2. EXPERIMENTAL

2.1. Preparation of Sb:SrF_2 Nanoparticles

The solid-state method was used to prepare SrF_2:Sb 0.0, 0.1, 0.15, 0.2, 0.25, 0.3 wt.% as follow accurately weighed in the required proportions and thoroughly mixed and ground using an agate slurry and pestle to convert into very fine powders. Acetone was used to help the solid compounds mix during the sample preparation process in relatively small quantities. The previous materials were ground and mixed with an agate mortar to ensure obtaining a homogeneous mixture after adding an amount of acetone in order to improve the homogeneous mixing process for it for about 15 minutes until the acetone dried. This process was repeated three consecutive times for each of the samples. After that, the resulting mixture was dried by heating it to a temperature of 100°C for a pe-

riod of time sufficient to ensure the removal of moisture. The samples were annealed at 350°C for 4 hours, after which the samples were gradually cooled in the heating oven to room temperature at a rate of 1°C/min.

2.2. Characterization

The crystallite structure and size of the synthesized nanoparticle samples were calculated using an x-ray powder diffractometer (XRD) (Philips-PW-1840) with a CoK_α radiation of 1.789 Å in a 2θ range of 20–80°. While the analysis of the chemical composition was carried out using Fourier transformation infrared (FT-IR model: Jasco Spectrum 4100 FT-IR) spectroscopy. The luminescence properties were studied using UV-Vis Spectroscopy.

3. RESULTS AND DISCUSSION

3.1. DTA Analysis

The DTA curve shown in Fig. 1, demonstrate the thermal behaviour of the system as it was scanned within a temperature range 0–1000°C. The ratio of 0.25 was chosen to study the thermal changes.

The DTA diagram shows exothermic effects. The first exothermic effect at 288°C indicates the entry of antimony into the crystal structure of strontium fluoride. The second exothermic effect at

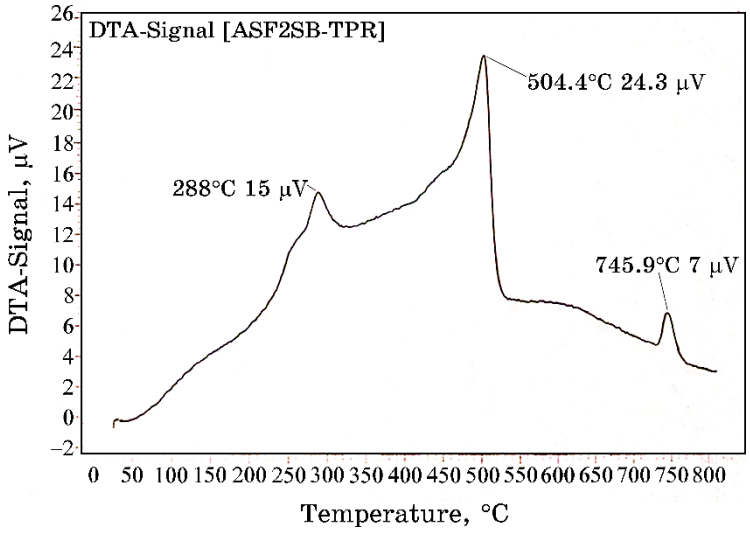

Fig. 1. DTA of SrF_2:Sb (0.25 wt.%).

504.4°C indicates the formation of antimony pentoxide Sb_2O_5. The third exothermic effect at 745.9°C indicates the formation of strontium oxide.

3.2. XRD Analysis

Figure 2 shows x-ray diagrams of strontium fluoride compound doped with antimony in different proportions. These diagrams are consistent with the reference card (SrF_2: 96-900-9044) for pure strontium fluoride with some displacement, indicating a clear change in the dimensions of the primary lattice cell as a result of the entry of antimony into the structure of strontium fluoride. The diagram SrF_2:0.3Sb shows a significant change in the structure in accordance with the reference card and this is explained by the formation of antimony pentoxide.

The average crystallite size was calculated using Scherrer's equation, which is expressed as follows [14]:

$$D = \frac{K\lambda}{\beta \cos\theta}, \tag{1}$$

where K is Scherrer's constant ($K = 0.89$ assuming spherical parti-

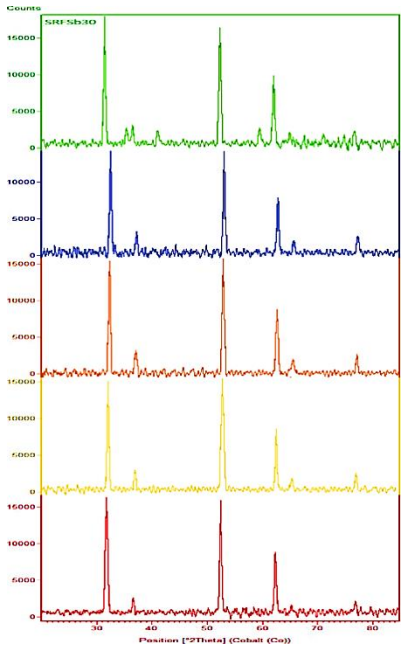

Fig. 2. XRD patterns of SrF_2:Sb nanoparticles.

cles), λ is the x-ray wavelength, β is the peak width at half maximum (*FWHM*), and θ is the Bragg's diffraction angle. The average crystal size was of 7.778 nm for SrF_2:0.25Sb.

3.4. FT-IR Spectroscopy

The FT-IR spectrum of SrF_2:Sb nanoparticles is presented in Fig. 3.

By comparing the infrared spectra of the compounds prepared

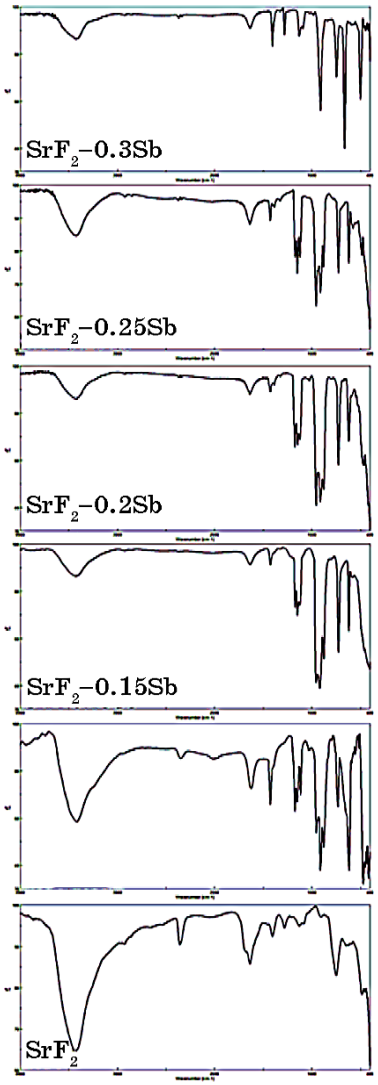

Fig. 3. FT-IR spectra of synthesized SrF_2:Sb nanoparticles.

with different proportions of antimony, it was found that new absorption bands appeared that were different from the absorption bands of the pure strontium fluoride compound. These bands appear at 469, 615, 728, 876, 953, 1115, 1147, 1172 cm^{-1}. These bands may be due to the vibration of the bonds according to the vibrational patterns: Sr–Sb–Sr, Sb–Sr–Sb, Sr–Sb–F, Sb–Sr–F, Sb–F–Sb, and F–Sb–F. This is evidence of the occurrence of a bond between the antimony atoms and the strontium fluoride, which confirms the entry of these atoms into the crystal structure of the compound.

As for the doping ratio (0.3), it was observed in the resulting spectrum that the previously formed bands disappeared, indicating the dissociation of antimony from strontium fluoride and the appearance of new absorption bands at wave numbers 414, 447 cm^{-1}

TABLE. The emission wavelength and the calculated energy gap.

	Wavelength	Energy gap
excitation	200	6.18
emission	310	3.99
emission	340	3.64
emission	355.4	3.48
emission	420	2.94
emission	451	2.74
emission	473	2.61
emission	495	2.50

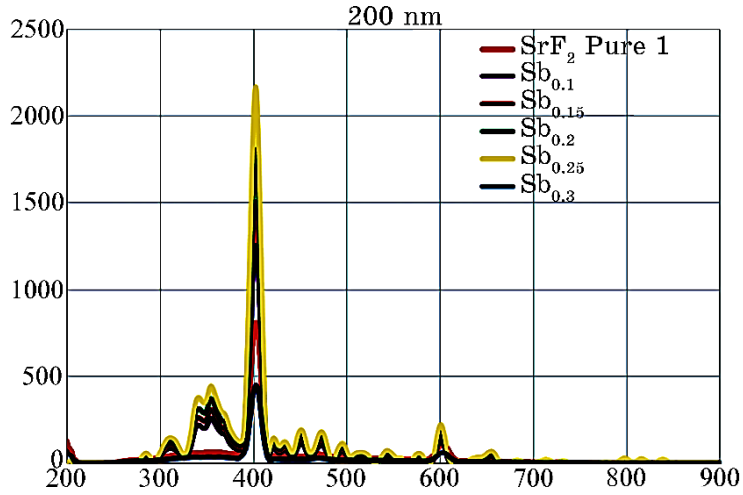

Fig. 4. Luminescence spectrum of SrF_2:Sb nanoparticles at 200 nm excitation wavelength.

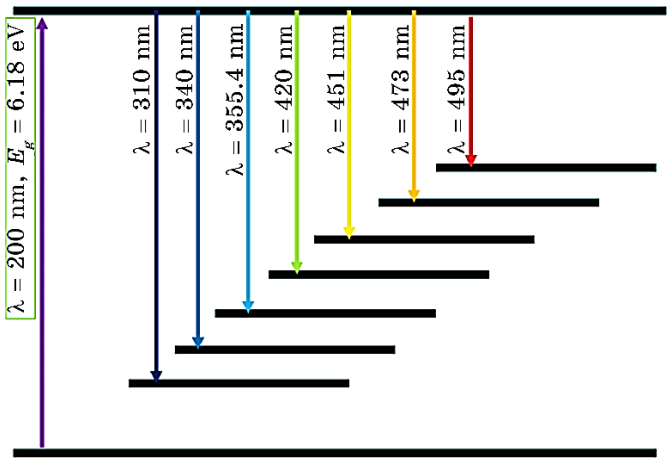

Fig. 5. The electronic transitions in the SrF_2:Sb.

due to the bonds Sb–O–Sb, O–Sb–O, and this is evidence of the formation of antimony oxide (Sb_2O_3).

3.3. The Luminescence Properties

The luminescence of the samples was measured using a UV-Vis spectroscopy, where the samples were excited at different wavelengths and the emission spectrum of these samples was recorded (Table).

Figure 4 shows the luminescence spectrum of the prepared samples with different doping ratios at 200 nm excitation wavelength.

These electronic transitions can be represented by the following diagram shown in Fig. 5.

CONCLUSION

SrF_2:Sb nanoparticles were successfully synthesized using soled state method. The resulting compounds were characterized using XRD techniques, which confirmed the size of nanoparticles, and IR spectroscopy. The photoluminescence was studied and have a clear fluorescence property.

REFERENCES

1. A. Ikesue, T. Kinoshita, K. Kamata, and K.J. Yoshida, *J. Am. Ceram. Soc.*, **78**, Iss. 4: 1033 (1995); https://doi.org/10.1111/j.1151-

2916.1995.tb08433.x
2. S. J. Pearton, D. P. Norton, K. Ip, Y. W. Heo, and T. Steiner, *Prog. Mater. Sci*, **50**, Iss. 3: 293 (2005); https://doi.org/10.1016/j.pmatsci.2004.04.001
3. S. Faÿ, L. Feitknecht, R. Schlüchter, U. Kroll, E. Vallat-Sauvain, and A. Shah, *Sol. Energy Mater. Sol. Cells*, **90**, Iss. 18–19: 2960 (2006); https://doi.org/10.1016/j.solmat.2006.06.003
4. W. Minrui, J. Wang, W. Chen, Y. Cui, and L. Wang, *Mater. Chem. Phys.*, **97**, Iss. 2–3: 219 (2006); https://doi.org/10.1016/j.matchemphys.2005.07.072
5. L. Su-Shia, J. Huang, and D. Lii, *Mater. Chem. Phys*, **90**, Iss. 1: 22 (2005); https://doi.org/10.1016/j.matchemphys.2004.08.040
6. M. Kaur, S. Bhattacharya, M. Roy, S. K. Deshpande, P. Sharma, S. K. Gupta, and J. V. Yakhmi, *Appl. Phys*, **A87**: 91 (2007); https://doi.org/10.1007/s00339-006-3858-8
7. Y. Ishikawa, Y. Shimizu, T. Sasaki, and N. Koshizaki, *J. Colloid. Interface Sci*, **300**, Iss. 2: 612(2006); https://doi.org/10.1016/j.jcis.2006.04.005
8. V. V. Pokropivny and M. M. Kasumov, *Tech. Phys. Lett.*, **33**: 44 (2007); https://doi.org/10.1134/S1063785007010129
9. G. P. Zhu, C. X. Xu, X. F. Wu, Y. Yang, X. W. Sun, and Y. P. Cui, *J. Electron. Mater.*, **36**: 494 (2007); https://doi.org/10.1007/s11664-006-0068-2
10. W. T. Yao, S. H. Yu, Y. Zhou, J. Jiang, Q. S. Wu, L. Zhang, and J. Jiang, *J. Phys. Chem. B*, **109**, Iss. 29: 14011 (2005); https://doi.org/10.1021/jp0517605
11. C. H. Loa, T. T. Tsung, and H. M. Lin, *J. Alloys Compd*, **434–435**: 659 (2007); https://doi.org/10.1016/j.jallcom.2006.08.217
12. J. K. Lung, J. C. Huang, D. C. Tien, C. Y. Liao, K. H. Tseng, T. T. Tsung, W. S. Kao, T. H. Tsai, C. S. Jwo, H. M. Lin, and L. Stobinski, *J. Alloys Compd*, **434–435**: 655(2007); https://doi.org/10.1016/j.jallcom.2006.08.213
13. A. A. Ashkarran, A. I. Zad, M. M. Ahadian, and S. A. Ardakani, *Nanotechnology*, **19**, Iss. 19: 195709 (2008); https://doi.org/10.1088/0957-4484/19/19/195709
14. J. Al-Ebraheem, M. N. Alkhoder, and R. H. Tulaimat, *Heliyon*, **10**, Iss. 2: 24652 (2024); https://doi.org/10.1016/j.heliyon.2024.e24652